Dictyostelid Cellular Slime Molds from the Russian Far East<!–<RunningTitle>Dictyostelid Slime Molds from the Russian Far East</RunningTitle>–>

Wenxiu Li, Yuhua Wei, Yue Zou, Pu Liu, Zhuang Li, Andrey A. Gontcharov, Steven L. Stephenson, Qi Wang, Shunhang Zhang, Yu Li

PII: S1434-4610(20)30061-4

DOI: https://doi.org/10.1016/j.protis.2020.125756

Reference: PROTIS 125756

To appear in: *Protist*

Received Date: 6 February 2020

Accepted Date: 5 August 2020

Please cite this article as: { doi: https://doi.org/

ORIGINAL PAPER

Dictyostelid Cellular Slime Molds from the Russian Far East

Running title: Dictyostelid Slime Molds from the Russian Far East

Wenxiu Li[a,1], Yuhua Wei[a,1], Yue Zou[a], Pu Liu[a,2], Zhuang Li[b], Andrey A. Gontcharov[c], Steven L. Stephenson[d], Qi Wang[a], Shunhang Zhang[a], and Yu Li[a,2]

[a]Engineering Research Center of Edible and Medicinal Fungi, Ministry of Education, Jilin Agricultural University, Changchun, People's Republic of China

[b]Shandong Provincial Key Laboratory for Biology of Vegetable Diseases and Insect Pests, College of Plant Protection, Shandong Agricultural University, Tai' an, People's Republic of China

[c]Institute of Biology and Soil Science FEB RAS, 100-letia Vladivostoka prospect, 159, Vladivostok, 690022, Russia

[d]Department of Biological Sciences, University of Arkansas, Fayetteville, Arkansas, USA

Submitted February 6, 2020; Accepted August 5, 2020

Monitoring Editor: Sandra Baldauf

[1]These authors contributed equally to this work.

[2]Corresponding authors; e-mails puliu1982@yahoo.com (P. Liu), fungi966@126.com (Y. Li).

Dictyostelid cellular slime molds (dictyostelids) are important soil microorganisms that feed mostly on bacteria in the soil and leaf litter layer. The Russian Far East is the easternmost part of Russia and thus is located in the Middle East of Siberia. In September 2018, 14 samples of mixed soil/humus were collected from the most southeastern portion of the Russian Far East, including Sakhalin Island, Ussuriysk and Vladivostok, and then processed for dictyostelids. Seven species in four genera were recovered. Four of these species (*Cavenderia fasciculata*, *Heterostelium tenuissimum*, *Dictyostelium longosporum* and *Polysphondylium patagonicum*) were recorded for the first time from Russia, and one species (*H. multibrachiatum* sp. nov.) in described herein as new to science.

Key words: Cellular slime molds; *Dictyostelium*, *Heterostelium*, *Polysphondylium*, *Cavenderia*, taxonomy.

Introduction

The dictyostelids (cellular slime molds) are a major assemblage within the organisms referred to as "slime molds" and belong to the supergroup Amoebozoa. They are associated primarily with decaying leaf litter, upper layers of the soil and animal dung. The dictyostelids are a common and widespread component of the soil microflora, where they feed on bacteria (Cavender and Raper 1965a, b). As bacterial predators, they potentially plasy important roles in soil ecology and promote soil and plant health by performing top-down control on ecosystem processes (e.g., decomposition) in which bacterial populations are involved (Romeralo et al. 2011).

Previous reports of dictyostelids in Russia are limited, with only one previous survey of dictyostelids carried out. Stephenson et al. (1997) reported six species of dictyostelids [*Dictyostelium mucoroides* Bref, *D. sphaerocephalum* Sacc & Marchal, *Cavenderia aureostipes* (Cavender) S. Baldauf, S. Sheikh & Thulin, *Raperostelium minutum* (Raper) S. Baldauf, S. Sheikh & Thulin, *Heterostelium pallidum* (Olive) S. Baldauf, S. Sheikh & Thulin and *H. tenuissimum* (H. Hagiw.) S. Baldauf, S. Sheikh & Thulin and *Polysphondylium violaceum* Bref] from soil samples collected in the region around the city of Magadan. This study compared data on the occurrence and distribution of dictyostelids in soils of western Alaska and eastern Russia. These two areas are located in portions of Asia and North America that were once linked by a land mass that has become known as Beringia.

Much of the Russian Far East, which displays relatively little variation in elevation, extends as far west as the edge of the Western Siberian Plateau. This region is mostly characterized by a temperate continental and fairly cold climate. Sakhalin Island has a continental monsoon climate and is located in the cold temperate zone, with short summers and six months of winter. Most of this island is mountainous, with two parallel ranges–the East and West Sakhalin Mountains–in the middle and southern portions, and the highest peak, Lopatina Mountain, has an elevation of 1609 m. Vladivostok is located in the eastern portion of the Eurasian continent on the southernmost point of the Amur Peninsula, with an elevation of 183 m. It is the most important city in the Far East of Russia. Ussuriysk, with an elevation of 33 m, supports a high diversity of animals and plants. There are no glaciers in this territory. Numerous rare plants occur at the edge of the city of Ussuriysk. These plants (e.g., *Panax ginseng*, *Acanthopanax senticosus*, *Schisandra chinensis* and *Actinidia chinensis* Planch) are uncommon in other regions of Asia (https://www.weatheronline.co.uk/reports/climate/Russia.htm). The soil samples for isolation of dictyostelids in this study were obtained at lower elevations and included several sites on Sakhalin Island and in the vicinity of Ussuriysk and Vladivostok. The overall purpose of the present study was to expand the body of

data available on the taxonomy and phylogeny of dictyostelids from the Russian Far East.

Results

Ten isolates representing seven species of dictyostelids were recovered from samples collected at the four localities in the Russian Far East (Table 1, Fig. 1). From these isolates, one new species (*Heterostelium multibrachiatum* sp. nov.) was isolated from two different collecting sites (L1 and L4). Four of the species recorded [*Cavenderia fasciculata* (F. Traub) S. Baldauf, S. Sheikh & Thulin, *H*. *tenuissimum, Dictyostelium longosporum* Hagiw and *Polysphondylium patagonicum* Vadell] are new records for Russia. Two of the species recorded (*C. aureostipes* and *P. violaceum*) had been reported previously. Phylogenetic studies based on the ribosomal small subunit (SSU) rRNA further support the taxonomic status of all seven species (Fig. 2). Isolates of all of these species have been deposited in the Herbarium of the Mycological Institute of Jilin Agricultural University (HMJAU), Changchun, China

Taxonomy and Molecular Phylogeny

Heterostelium multibrachiatum Y. Li, P. Liu et Wen. X. Li, sp. nov.

MycoBank accession number. MB833469

When cultured at 23 °C on non-nutrient agar with *Escherichia coli*, sorocarps (Fig. 3A–C) are typically loose or tightly clustered, sometimes solitary, erect or inclined to prostrate, phototropic, 0.71–7.89 mm high, with 1–13 nodes, bearing 2–8 branches, with an average of up to 12 branches, branch length is uneven, 160.79–629.42 μm. Sorophores colorless, sinuous, sometimes undulate, sturdy, tapered, consisting of 1–

2 tiers of cells, 11.52–15.74 μm. Terminal segment occasionally short, internode segments 184.64–443.42 μm, bases (Fig. 3I–L) round to conical with a dense covering of mucilage, 17.36–48.49 μm, often two cells, sometimes compound; tips (Fig. 3H) acuminate, 5.68–11.62 μm. Branches (Fig. 3M) delicate, 64.64–109.33 μm, bases of branches nearly expanded, 5.43–5.73 μm, branch tips acuminate, 2.14–2.84 μm. Sori globose, pale, terminal sori 70.23–149.86 μm in diameter, lateral sori 31.01–99.97 μm in diameter. Lateral sori form earlier than terminal sori. Spores (Fig. 3N–O) hyaline, elliptical, 4.62–6.24 × 1.71–3.69 μm, with consolidated polar granules. The cell aggregations (Fig. 3D–E) radiate in pattern, usually centralized, pseudoplasmodia (Fig. 3F–G) not migrating without sorophore formation.

Etymology. Referring to the sorocarps with multiple branches.

Holotype. HMJAU MR316 (5916lun), isolated from a soil sample (S5916, pH 7.06) collected in a mixed forest near Ussuriysk, Primorsky Krai, Russia (43°69'43"N, 132°15'29"E), located at an elevation of approximately 100.9 m, on 19 September 2018.

GenBank Accession Number. MN752217.

Commentary. Typically, this species has more branches per node near the apex of the sorophore, with one separate branch usually occurring in the middle of two whorls. The lateral sori on the separate branch are usually very small (25.81–34.59 μm in diameter). Molecular phylogeny based on SSU rRNA supported the position of this species in the genus *Heterostelium.* (Fig. 2). This species forms a clade with *H. pseudocandidum* (H. Hagiw) S. Baldauf, S. Sheikh & Thulin. (Hagiwara 1989; Sheikh et al. 2018). The nodes of *H. multibrachiatum* are 1–13, whereas in *H. pseudocandidum* the nodes are 1–5. The sorophore base in *H. multibrachiatum* is round to conical and with a supported structure, whereas it is clavate to round in *H. pseudocandidum*. The size of the sori in *H. multibrachiatum* (70.23–149.86 μm in diameter) is larger than the corresponding figure in *H. pseudocandidum* (20–110 μm in diameter). The spore size of *H. pseudocandidum* (6.2–7.9 × 3.0–3.7 μm) is larger than is the case for *H*. *multibrachiatum* (4.62–6.24 × 1.71–3.69 μm).

Other specimens examined. HMJAU MR317 (5904lun), isolated from a soil sample (S5904, pH 4.45) collected in a mixed forest, Korsakovsky District, Sakhalin Island, Russia (46°83'07''N, 143°17'05''E), located at an elevation of approximately 2.5 m, on 13 September, 2018.

GenBank Accession Number. MN752218.

Polysphondylium patagonicum Vadell et al., Mycologia 103: 113 (2011)

When cultured at 23 °C on non-nutrient agar with *E. coli,* sorocarps (Fig. 4A–B) are solitary to clustered, erect or prostrate, frequently coremiform, phototropic, varying in size, about 1.22–5.91 mm high. Sorophores sigmoid, curved, slightly violet to bluish-wine. Developing markedly elongated branches (Fig. 4E) when prostrate. Upper sorophores (Fig. 4F) with one tier of cells. Bases (Fig. 4G) clavate, 17.62–26.76 µm, bearing 1–5 unevenly spaced nodes of lateral branches, mostly 2–5 branches per node; branches often 173.47–461.82 µm. Large branches in a node are at an angle of 90 degrees with respect to the sorocarp, then recurved. Sori globose, light vinaceous to wine, terminal sori 76.78–180.22 µm in diameter. Lateral sori 45.53–93.38 µm in diameter. Spores (Fig. 4H) elliptical, commonly 5.21–8.42 × 2.56–3.99 µm, with conspicuous refractile, vinaceous, consolidated polar granules. The cell aggregation (Fig. 4C) radiate in pattern, with few relatively large streams, pseudoplasmodia (Fig. 4D) not migrating without sorophore formation.

Cultures examined. HMJAU MR318 (strain 5912zi). Isolated from a soil sample (S5912, pH 5.35, elevation 17.7 m, coordinates 46°59'09''N, 143°18'05''E) from a coniferous forest, collected on 15 September, 2018 in the Korsakovsky District, Sakhalin Island, Russia.

GenBank Accession Number. MN752219.

Known distribution. Patagonia, Argentina, and Russia.

Commentary. This species is reported for the first time from Russia. Molecular data from the SSU rDNA phylogeny support the placement of this species in the genus *Polysphondylium* (Sheikh et al. 2018) (Fig. 2). This species forms a clade with *P.*

fuscans Perrigo and *P. patagonicum* (GenBank Accession Number. GQ496156.1) (Perrigo et al. 2013; Vadell et al. 2011). The sizes of the terminal sori (76.78–180.22 μm in diameter) and lateral sori (45.53–93.38 μm in diameter) of *P. patagonicum* in our study are much smaller than *P. fuscans* (130–240 μm in diameter, 40–130 μm in diameter) (Perrigo et al. 2013). The color of the sori in *Polysphondylium patagonicum* is light vinaceous to wine, whereas the color is purple in *P. fuscans* (Perrigo et al. 2013). *P. patagonicum* resembles *P. violaceum* (Cavender et al. 2002) because of the colored sori and branches but differs from *P. violaceum* largely with respect to the branch style and the color of the sori. When the sorocarps are prostrate, no whorls and larger upright branches are formed in the sorocarps of *P. patagonicum* (Vadell et al. 2011). Sori color of *P. patagonicum* is lighter than that of *P. violaceum,* varying from light vinaceous to wine. The number of whorls in *P. patagonicum* (1–5) is lower than the number in *P. violaceum* (3–8).

Cavenderia fasciculata (F. Traub et al.) S. Baldauf, S. Sheikh & Thulin, Protist 169:19 (2018)

When cultured at 23 °C on non-nutrient agar with *E. coli,* sorocarps (Fig. 5A–B) are clustered to solitary, semierect to prone, 1.88–3.05 mm high, phototropic. Sorophores delicate, colorless, consisting of single or double tiers of cells occasionally branched, comparatively thin, tapered from clavate or plane bases (Fig. 5I) (10.76–17.93 μm) to capitate tips (Fig. 5H) (4.25–9.45 μm). Sori globose to citriform, milk-white to cream-colored, mostly 95.41–231.82 μm in diameter. Spores (Fig. 5J) mostly elliptical to oblong, sometimes spherical, commonly 5.02–6.07 × 2.19–3.03 μm, with prominent polar to subpolar granules, the latter sometimes larger and monopolar. The cell aggregation (Fig. 5C–E) has a distinct cell flow, which is later divided into small clusters to form clustered spores. Pseudoplasmodia (Fig. 5F–G) migrate with stalk formation, producing clustered sorogens.

Cultures examined. HMJAU MR319, HMJAU MR320 (strain 5913, strain 5913cu). Isolated from a soil sample (S5913, pH 6.12, elevation 52 m, coordinates

43°19'37"N, 131°92'12"E) from a mixed forest collected on 19 September 2018 in Ussuriysk, Primorsky Krai, Russia.

GenBank Accession Number. MN752220, MN752221.

Known distribution. Switzerland, Denmark, France, United States, New Zealand, and Russia.

Commentary. *Cavenderia fasciculata* is widespread in Europe, Oceania and North America (Cavender et al. 2002; Traub et al. 1981), but this is the first time it has been recorded from Russia. The species is characterized by its clustered sorocarps which also resemble those of *Dictyostelium mucoroides*. Molecular data from SSU rRNA supports the placement of this species in the genus *Cavenderia* (Sheikh et al. 2018) (Fig. 2). This species forms a clade with *C. fasciculata* (GenBank Accession Number. AM168086.1) and *C. antarctica* (Cavender et al.) S. Baldauf, S. Sheikh & Thulin (Sheikh et al., 2018; Cavender et al., 2002). The size of sorocarps of the isolate obtained in our study is 1.88–3.05 mm, whereas the size of those of *C. antarctica* is only 0–1.5 mm (Cavender et al. 2002). The clavate bases with an enlarged terminal cell and smaller supporter cells found in *C. antarctica* (Cavender et al. 2002) are lacking in *C. fasciculata.*

Heterostelium tenuissimum (H. Hagiw.) S. Baldauf, S Sheikh & Thulin, Protist 169: 18 (2018)

When cultured at 23 °C on non-nutrient agar with *E. coli*, the sorocarps (Fig. 6A–B) are usually solitary but sometimes gregarious, erect or prostrate, with 5–17 nodes, each node bearing 3–6 branches, not phototropic. Sorophores colorless, delicate, sinuous, 2.76–10.43 mm high, arising from clavate or round bases (Fig. 6F–G), with two tiers of cells, gradually tapering from 12.35–31.44 µm near the base to 5.60–6.88 µm near the acuminate tip (Fig. 6E), simple; terminal segments 300.27–438.72 µm, internodes mostly 171.99–306.87 µm. Branches (Fig. 6H) straight or somewhat curved, arising from clavate bases, gradually tapering from 3.09–9.43 µm near the base to 1.37–4.12 µm near the tip. Terminal sori white, globose, mostly 45.77–111.08

μm in diameter. Lateral sori globose, mostly 28.84–68.17 μm in diameter. Spores (Fig. 6I) elliptical to oblong, usually 1.6–2.4 times longer than broad, smooth, mostly 5.15–7.88 × 2.15–3.86 μm, with polar granules. The cell aggregation (Fig. 6C) is radial, pseudoplasmodia (Fig. 6D) not migrating without sorophore formation.

Cultures examined. HMJAU MR321 (strain 5911lun). Isolated from a soil sample (S5911, pH 5.81, elevation -3 m, coordinates 46°60'05"N, 143°18'09"E) from a coniferous forest, collected on 15 September, 2018 in the Korsakovsky District, Sakhalin Island, Russia.

GenBank Accession Number. MN752222.

Known distribution. United States, Guatemala, Japan, China, and Russia.

Commentary. *Heterostelium tenuissimum* has been reported previously from North America, Europe and Asia (Hagiwara 1989), but this is the first time it has been reported from Russia. The species is characterized by the large number of whorls, short branches, and small sori. SSU rRNA phylogeny places this species in a highly supported clade together with *H. pallidum* (Sheikh et al. 2018) and *H. tenuissimum* (GenBank Accession Number. AY040339.1) (Fig. 2). The number of sorocarp nodes in the isolate obtained in our study is 5–17, whereas the number in *Heterostelium pallidum* is only 1–11 (Olive 1901). The size of the sori in *H. tenuissimum* reported herein (45.77–111.08 μm in diameter) is much smaller than that those of *H. pallidum* (150–260 μm in diameter). The terminal sori of our isolate are slightly larger than the original report of *H. tenuissimum* (30–80 μm in diameter) (Liu and Li 2017).

Dictyostelium longosporum H. Hagiw., Bull. Natl. Sci. Mus., Tokyo, B, 9: 55 (1983). When cultured at 23 °C on non-nutrient agar with *E. coli*, the sorocarps (Fig. 7A–B) are usually solitary, unbranched or occasionally with small branches, phototropic, mostly erect, sometimes prostrate. Sorophores colorless, sinuous, solid, 0.87–3.67 mm high, gradually tapering from bases to tips, bases (Fig. 7F) round to expanded, 5.16–22.40 μm, tips (Fig. 7E) capitate, 3.00–11.26 μm. Sori white, globose, 49.47–389.50 um in diameter. Spores (Fig. 7G) hyaline, ellipsoid or oblong, usually 1.9–2.4

times longer than broad, smooth, mostly 6.44–8.90 × 2.88–4.38 µm, without polar granules. The cell aggregations (Fig. 7C) have radiate streams. Pseudoplasmodia (Fig. 7D) not migrating without stalk formation.

Cultures examined. HMJAU MR322 (strain 5916). Isolated from a soil sample (S5916, pH 7.06, elevation 100.9 m, coordinates 43°69'43''N, 132°15'29''E) from a mixed forest collected on 19 September, 2018 in Ussuriysk, Primorsky Krai, Russia.

GenBank Accession Number. MN752223.

Known distribution. Nepal, China, and Russia.

Commentary. *Dictyostelium longosporum* was first reported from Nepal (Hagiwara 1983) and then recorded from China (Liu and Li 2017) and Russia in the present study. It is characterized by its medium-sized but strong sorocarps, capitate tips on the top of the sorophores and the elongated spores. The size of sorocarps in the isolate recovered in our study is somewhat smaller than the previous report. This species belongs to dictyostelid Group 4 (Sheikh et al. 2018) in an SSU rRNA phylogeny (Fig. 2). It forms a clade together with *Dictyostelium valdivianum* Vadell (Fig. 2). Morphologically, *D*. *longosporum* can be differentiated from *D*. *valdivianum* by its round bases, capitate tips without a dense covering of mucilage, the curved bases and the flexuous tips in *D*. *valdivianum* (Vadell et al. 2011). The sori size in *D*. *longosporum* (49.47–389.50 µm in diameter) is larger than that of *D*. *valdivianum* (50–220 µm in diameter) (Vadell et al. 2011). The streams of the cell aggregations are not prominent in *D*. *valdivianum* (Vadell et al. 2011) but obvious in *D*. *longosporum*.

Polysphondylium violaceum Bref., Untersuch. Gesammt. Mykol. 6: 5 (1884).

When cultured at 23 °C on non-nutrient agar with *E. coli*, sorocarps (Fig. 8A–C) are solitary, sometimes gregarious, erect to semierect or prostrate, 2.17–7.32 mm high, strongly phototropic, usually with 4–9 nodes, with 2–6 branches per node. Terminal segments 516.41–950.74 µm; internode segments 288.16–665.38. µm. Sorophores pale violet, sinuous, mostly compound, sometimes simple, bases (Fig. 8G–H) clavate

to round, 16.74–48.49 μm near the base, tips (Fig. 8F, J) clavate, usually 6.79–19.26 μm near the apex. Branches (Fig. 8I) 113.47–256.15 μm, branch bases clavate, 9.20–20.88 μm at the thickest part; branch tips clavate, 4.27–8.50 μm. Sori globose, violaceous or light purple; terminal sori 90.56–166.64 μm in diameter; lateral sori 61.88–88.56 μm in diameter. Spores (Fig. 8K) hyaline, elliptical to oblong, mostly 4.25–8.15 × 2.31–4.74 μm, usually with consolidated granules but sometimes unconsolidated. The cell aggregations (Fig. 8D) are radial, pseudoplasmodia (Fig. 8E) not migrating without sorophore formation.

Cultures examined. HMJAU MR323, MR324 (strain 5913zi, strain 5915zi). Isolated from soil (S5913, pH 6.12, elevation 52 m, coordinates 43°19'37''N, 131°92'12''E; S5915, pH 7.08, elevation 184.4 m, coordinates 43°69'04''N, 132°15'46''E) samples from a mixed forest collected on 19 September, 2018 in Vladivostok and Ussuriysk, Primorsky Krai, Russia.

GenBank Accession Number. MN752224, MN752225.

Known distribution. Japan, United States, Canada, India, Nepal, Yugoslavia, Singapore, Thailand, Philippines, Germany, Malaysia, Uganda, Mexico, Costa Rica, Indonesia, Kenya, Tanzania, Switzerland, Spain, China, and Russia.

Commentary. The typical characteristics of *Polysphondylium violaceum* are the violet sorocarps and the radial pseudoplasmodia. This species is cosmopolitan and thus found throughout the world. It often produces irregularly and profusely branched sorocarps. A SSU rRNA phylogeny placed these two strains in a highly supported clade together with *P. fuscans* and *P. patagonicum* (Fig. 2). Morphologically, *P. fuscans* is most similar to *P. violaceum,* but it differs primarily in the lighter initial pigmentation of the sori, smaller number (1–3) of nodes and larger spore size (6.0–8.5 × 3.0–4.0 μm) (Perrigo et al. 2013).

Cavenderia aureostipes (Cavender) S. Baldauf, S. Sheikh & Thulin. Protist 169: 18 (2018)

When cultured at 23 °C on non-nutrient agar with *E. coli,* sorocarps (Fig. 9A) are usually solitary, commonly 3.99–6.22 mm high, sometimes clustered, erect or semierect, typically branched, strongly phototropic; easily lodging, sorophores golden-yellow, with pigmentation enhanced by dark incubation, usually bearing 10–25 irregular lateral branches, often 427.87–809.23 μm, sturdy, tapering from 20.71–28.99 μm, near the base to 7.42–10.63 μm at the tips; bases (Fig. 9F) clavate, two or multiple tiers of cells, tips (Fig. 9D–E) obtuse; sori globose, white, terminal; sori 130.85–249.69 μm in diameter, lateral sori 35.78–90.25 μm in diameter; spores (Fig. 9G) elliptical to slightly reniform, mostly 2.12–3.89 × 4.29–7.30 μm, with prominent polar granules. The cell aggregation (Fig. 9B) with radiate streams, pseudoplasmodia (Fig. 9C) not migrating without sorophore formation.

Cultures examined. HMJAU MR325 (strain 5914jinbing). Isolated from a soil sample (S5914, pH 6.85, elevation 52 m, coordinates 43°19'37''N, 131°92'12''E) from a mixed forest collected on 18 September, 2018 in Vladivostok, Primorsky Krai, Russia.

GenBank Accession Number. MN752226.

Known distribution. Switzerland, United States, Japan, India, Nepal, China, and Russia.

Commentary. *Cavenderia aureostipes* is a widely distributed species which occurs mostly in fertile soils or humus. A SSU rRNA phylogeny places this species in a highly supported clade together with *C. aureostipes* (GenBank Accession Number. AM168083.1) (Fig. 2). The identification of this species can be achieved through the following aspects: the pale yellow sorophores, the irregular branching and the milky sori. The base of sorophores in the isolate recovered in the present study (20.71–28.99 μm) are thinner than those cited in published descriptions, where the sizes reported are 25–30 μm or 10–80 μm (Cavender et al. 2002; Traub et al. 1981).

Discussion

For a long time, the traditional classification used for dictyostelids recognized four genera based on their morphological characteristics. These were *Dictyostelium, Polysphondylium, Actyostelium* and *Coenonia* (Olive 1901). More recently, dictyostelids have been classified more precisely according to their molecular phylogeny based on SSU rRNA sequences, and 12 different genera are currently recognized (Medlin et al. 1988; Sheikh et al. 2018). In the present study, the seven species isolated were all classified both by morphological and phylogenetic characteristics. From the phylogenetic tree based on SSU rRNA sequences (Fig. 2), *Heterostelium multibrachiatum*, *Cavenderia aureostipes* and *C. fasciculata* are all the sole member of their respective monophyletic groups. However, *P. violaceum* is in a paraphyletic assembly; *P. patagonicum* is paraphyletic with respect to *P. fuscans* collected from Sweden; *D. longosporum* forms a clade with respect to *D. valdivianum* plus an undefined *Dictyostelium* clade; and *H. tenuissimum* is paraphyletic if *H. pallidum* PPHU8 was properly identified. A number of studies have demonstrated that species of dictyostelids can be distinguished by a combination of molecular phylogeny and morphology (Sheikh et al. 2018; Vadell et al. 2018).

The diversity and distribution of dictyostelids are related to environmental conditions such as temperature, humidity, pH, elevation and latitude (Romeralo et al. 2011). Swanson et al. (1999) suggested that pH and elevation are important drivers of dictyostelid richness throughout the world. However, Paillet et al. (2010) found that the higher the elevation, the higher the biodiversity of dictyostelids, whereas Landolt et al. (2006) observed a negative effect of elevation on dictyostelid abundance and a positive effect on species richness. In our study, the elevation of collecting sites ranged from -10 m to 185 m, and we found that ten of the fourteen soil samples collected from relatively lower elevation (-10–17.7 m) areas of Sakhalin Island yielded only three species. These results suggested that perhaps the relatively lower elevations are not suitable for the growth of dictyostelids. The other four species in our study were isolated from soil samples collected from relatively higher elevations (52–184.4 m) compared with those from Sakhalin Island, although the absolute

difference in elevation was much less than what was considered in the study by Landolt et al. (2006).

Leitner (1987) made some observations of three species of dictyostelids with respect to the pH of forest soil and found that *Dictyostelium mucoroides* and *Cavenderia fasciculata* were more prevalent in deciduous forests with neutral or slightly alkaline soils, while *Raperostelium minutum* was more common in deciduous forest soils which were acidic (ca. pH 5.0). Moreover, Lauber et al. (2009) also analyzed various soil characteristics such as mean annual temperature, soil moisture deficit, soil texture and pH. Their data suggested that pH was the most important factor in determining the bacterial community structure and diversity. Diversity of dictyostelids was highest in soils with a nearly neutral pH in that study. There are some publications in which the pH of soil samples was recorded, and the values ranged from 3.5 to 7.6 (Cavender et al. 1995; Leitner 1987). In our study, the pH of soil mostly ranged from 4.5 to 7.1. The seven species reported herein were isolated from soils with pH values (pH 5.5–7.1) close to neutrality except for the new species, which was isolated both from soils with a near neutral (pH 7.1) as well as acidic soils (pH 4.5).

Most previous studies of dictyostelids have been carried out in middle–high (30°–60°N, 30°–60°S) (Cavender et al. 2002, 2005; Landolt et al. 2008; Liu and Li 2011; Liu et al. 2019b; Paillet and Satre 2010; Romeralo et al. 2009; Stephenson et al. 1997; Vadell et al. 2011; Zhao et al. 2017) or high latitudes (60°–90°N) (Cavender 1978; Landolt et al. 1992; Perrigo et al. 2013; Romeralo et al. 2010; Stephenson et al. 1991, 1997), with only a few reports from low latitudes (0°–30°N, 0°–30°S) (Cavender et al. 2013; Landolt et al. 2008; Liu et al. 2019a, c; Vadell et al. 2018). Our study sites are located at latitudes 43°–47°N, and thus belong to the middle–high latitudes. There are fourteen species [*C. aureostipes*, *D. sphaerocephalum, D. giganteum* B. N. Singh, *D. mucoroides, D. globisporum* Li Y & Liu P*, D. crassicaule* H. Hagiw*,* C. *fasciculoidea* (Vadell et al.) S. Baldauf,S. Sheikh & Thulin , *D. gargantuum* Vadell et al*, D. valdivianum, Polysphondylium patagonicum, Cavenderia*

antarctica , R. australe (Cavender et al.)S. Baldauf, S. Sheikh & Thulin, *C. fasciculata and P. pallidum*] of dictyostelids which have been reported from the same latitude range (40°–47°N, 40°–47°S) (Cavender et al. 2002; Paillet and Satre 2010; Vadell et al. 2011; Zhao et al. 2017). Only three species, *P. patagonicum* (Vadell et al. 2011), *C. fasciculata* (Cavender et al. 2002), and *C. aureostipes* (Paillet and Satre 2010), were recorded in the present study.

There are five islands from which dictyostelids were specifically examined until now. Three species of dictyostelids were recorded from Sakhalin Island in the present study. The total species' numbers from other reports (Stephenson et al. 2008; Liu et al. 2019c; Swanson et al. 2004; Landolt and Wong 1998) are one, three, four and 19 plus one variety, respectively, for Macquarie Island in the Subantarctic, Ascension Island in the mid-Atlantic Ocean, Christmas Island in the Indian Ocean and Hawaii Island in the central Pacific Ocean. The number of dictyostelids on Hawaii Island was significantly higher than for the others. Clearly, the dictyostelids of other small oceanic islands need to be investigated in more detail, the island habitats might be significant to dictyostelids.

In the new classification system (Sheikh et al. 2018), *Polysphondylium* was assigned to the *"violaceum"* complex. In our study, two strains of *P. violaceum* were obtained for the second time in Russia, with first record from Russia in 1997 (Stephenson et al. 1997). Moreover, one strain of *P. patagonicum* was obtained for the first time in the northern hemisphere. This species was named after being discovered in Patagonia (Vadell et al. 2011) but has not been reported since then. This study is the second report of dictyostelids from the Russian Far East; however, it is the first intensive survey of dictyostelids for Sakhalin Island, Ussuriysk and Vladivostok, Russia. Only two species (*C. aureostipes* and *P. violaceum*) were reported from the Russian Far East by Stephenson et al. (1997). Clearly, studies of dictyostelids in Russia are limited; further investigations of this group of organisms need to be carried out.

Methods

Sampling: Samples were collected in different types of vegetation, with the actual sampling sites randomly selected. Each sample was placed in a plastic ziplock bag, sealed, and the bag numbered and marked with the latitude and longitude, elevation, date and vegetation type. Each bag contained approximately 50 g of soil. Fourteen samples of soil were collected from four localities in the Russian Far East (Fig. 1) in September 2018. Ten samples of soil were collected from Sakhalin Island (eight from locality L1 and two from locality L2), two from Vladivostok (locality L3) and two from Ussuriysk (locality L4).

Sakhalin Island, located in the cold temperate zone, is characterized by short summers and six months of winter. The average temperature in winter is between -19 °C to -24 °C, but the lowest temperature in the north can reach -40 °C. Several parts of the island have been frozen for an extended period of time. The annual precipitation is 500-1200 mm. Korsakovsky (locality L1, 46°38'N, 142°46'E) is in the southern portion of Sakhalin Island, where it is located on the northern coast of the Bay of Aniwa (Yating Bay). Dolinsky (locality L2, 47°27'N, 142°75'E) is located 43 kilometers north of the South Saharinsk Peninsula. The climate is temperate continental and humid. The annual average precipitation is comparable to that of Sakhalin Island (https://www.weatheronline.co.uk/reports/climate/Russia.htm).

Vladivostok (L3, 43°19'N, 131°92'E) is the southernmost point on the Amur temperature is 8.38 °C, the average low temperature is 1.38 °C, and the average precipitation is 797 mm (https://www.weatheronline.co.uk/reports/climate/Russia.htm).

Ussuriysk (locality L4, 43°69'N, 132°15'E) is located between the Sikhote Mountains, the Changbai Mountains and Xingkai Lake. To the west, it is near Dongning in China, and to the south, it is 100 kilometers from Vladivostok. The coordinates are 43°48'N, 131°57'E. It represents the intersection of the Suifenhe,

Lakoffga and Suptiga rivers. Ussuriysk is located in the Eurasia and bordered on the east by the largest ocean on the earth. The average temperature in September is 15–17 C and the average precipitation is 590 mm (https://www.weatheronline.co.uk/reports/climate/Russia.htm).

Isolation and cultivation: The isolation methods used in the present study followed those described by Cavender and Raper (1965a) and are briefly summarized herein. A portion (10 grams) of each soil sample was mixed with 90 mL of distilled water and shaken at 280 rpm/min at 23 C for two minutes to prepare an initial soil suspension of 1:10. The pH of each suspension was determined using a portable pH meter. Afterwards, 5 mL of the soil suspension was mixed with 7.5 mL of sterile water to make a soil suspension of 1:25. Then, 0.5 mL of the soil suspension was uniformly spread over the surface of a hay infusion agar medium using an applicator. This was followed by adding 0.4 mL of a suspenstion of *Escherichia coli*, which was spread evenly over the surface of the agar. Five duplicate plates were prepared for each sample and incubated in an incubator at 23 °C with a 12 h light and dark cycle. After two to three days, the plates were examined and any dictyostelids observed were recorded. The isolates appearing in the plates were purified and cultivated for taxonomic studies on non-nutrient water agar plates with *Escherichia coli* pregrown for 12 to 24 h. Spores from these isolates were frozen in HL5 media (Cocucci and Sussman 1970) and stored at -80 °C in the Herbarium of the Mycological Institute of Jilin Agricultural University (HMJAU), Changchun, China.

Morphological observations: In the primary isolation plates, the location of each early aggregating clone and sorocarp(s) that developed was marked. The characteristic stages in the life cycle, including cell aggregation and the formation of pseudoplasmodia and sorocarps, were observed under a Zeiss dissecting microscope (Axio Zoom V16) with a 1.5× objective and 10× ocular. Slides with sorocarps were prepared with water as the mounting medium. Features of spores, sorophores, and sorocarps were observed and measured on the slides by using a Zeiss light microscope (Axio Imager A2), with an 10x ocular and 10, 40, and 100x

(oil) objectives. Photographs were obtained with a Zeiss Axiocam 506 color microscope camera.

DNA isolation, PCR amplification, sequencing and phylogenetic analysis: The molecular methods used in the present study followed those described by Liu et al. (2019c). The spores of all ten isolates being studied were collected with a sterile tip and mixed with the lysis buffer of the MiniBEST universal genomic DNA extraction kit ver.5.0 (TaKaRa, Japan) according to the manufacturer's protocol. The genomic DNA solution was used directly for the SSU PCR amplification using the primers 18SF-A (AACCTGGTTGATCCTGCCAG) and 18SR-B (TGATCCTTCTGCAGGTTCAC) (Medlin et al. 1988). PCR products were sent to Sangon Biotech Co., Ltd. (Shanghai, China), for sequencing. Sequences obtained were deposited in the GenBank database.

The ten newly generated sequences were checked and then submitted to GenBank. All the sequences of closely related species were downloaded from GenBank for phylogenetic analysis to determine their phylogenetic relationships with other taxa in the group. The SSU sequences of the seven new taxa were aligned with sequences from eight genera (Table 2). The SSU rRNA sequences were aligned and compared using the program MUSCLE v.3.6 (Edgar 2004a, b) and then manually adjusted and trimmed in MEGA 7.0 (Kumar et al. 2016). Maximum likelihood (ML) analyses were carried out using RAxML v7 (Stamatakis 2006). In the ML analyses, the best-fit substitution models were estimated using the GTR submission model and a gamma correction for rate variation among sites (GTRGAMMA), using the CIPRES server. The statistical support of clades was assessed with 1,000 rapid-bootstrap (BS) replications.

Authors' contributions

WxL, YhW, YZ, ZL, ShZ, AAG and QW carried out the research, WxL wrote the manuscript, YL and PL designed the research, SLS and PL revised the manuscript. All authors read and approved the final version of the manuscript.

Conflict of Interest

No.

Acknowledgements

This work was supported by funding supplied by the National Natural Science Foundation of China (No. 31870015) and the Science and Technology Development Program of Jilin Province (No. 20200801068GH and 20180414079GH). We thank two anonymous reviewers and editor Prof. Sandra L. Baldauf for their valuable comments and valuable reviews relating to this manuscript.

References

Cavender JC (1978) Cellular slime molds in tundra and forest soils of Alaska including a new species, *Dictyostelium septentrionalis*. Can J Bot **56**:1326–1332

Cavender JC, Raper KB (1965a) The Acrasieae in Nature. I. Isolation. Am J Bot **52**:294–296.

Cavender JC, Raper KB (1965b) The Acrasieae in Nature. II. forest soil as a primary habitat. Am J Bo **52**:297–302

Cavender JC, Cavender-Bares J, Hohl HR (1995) Ecological distribution of cellular slime molds in forest soils of Germany. Bot Helv **105**:199–219

Cavender JC, Stephenson SL, Landolt JC, Vadell EM (2002) Dictyostelid cellular slime moulds in the forests of New Zealand. New Zeal J Bot **40**:235–264

Cavender JC, Vadell E, Landolt JC, Stephenson SL (2005) New species of small dictyostelids from the Great Smoky Mountains National Park. Mycologia **97**:493–512

Cavender JC, Vadell EM, Landolt JC, Winsett KM, Stephenson SL, Rollins AW, Romeralo M (2013) New small dictyostelids from seasonal rainforests of Central America. Mycologia **105**:610–635

Cocucci SM, Sussman M (1970) RNA in cytoplasmic and nuclear fractions of cellular slime mold amebas. J Cell Biol **45**:399–407

Edgar RC (2004a) MUSCLE: a multiple sequence alignment method with reduced time and space complexity. BMC Bioinformatics **5**:113

Edgar RC (2004b) MUSCLE: multiple sequence alignment with high accuracy and high throughput. Nucleic Acids Res **32**:1792–1797

Hagiwara H (1983) Four new species of dictyostelid cellular slime molds from Nepal. Bull Natl Sci Mus Tokyo Ser B **9**:149–158

Hagiwara, H (1989) The taxonomic study of Japanese dictyostelid cellular slime molds. Natl Sci Mus Press, Tokyo, 131 p

Kumar S, Stecher G, Tamura K (2016) MEGA7: Molecular Evolutionary Genetics Analysis version 7.0 for bigger datasets. Mol Biol Evol **33**:1870.

Landolt JC, Wong GJ (1998) Dictyostelid cellular slime molds from Hawaii. Pacific Sci **52**:98–103

Landolt JC, Stephenson SL, Cavender JC (2006) Distribution and ecology of dictyostelid cellular slime molds in Great Smoky Mountains National Park. Mycologia **98**:541–549

Landolt JC, Cavender JC, Stephenson SL, Vadell EM (2008) New species of dictyostelid cellular slime moulds from Australia. Austr Syst Bot **21**:50–66

Landolt JC, Stephenson SL, Laursen GA, Densmore R (1992) Distribution patterns of cellular slime molds in the Kantishna Hills, Denali National Park and Preserve, Alaska, U.S.A. Arctic Alpine Res **24**: 244–248

Lauber CL, Hamady M, Knight R, Fierer N (2009) Pyrosequencing-based assessment of soil pH as a predictor of soil bacterial community structure at the continental scale. Appl Environ Microbiol **75**:5111-5120

Leitner A (1987) Acrasiales in geschädigten Wäldern. Staatsexamensarbeit. Universität Konstanz, 91 p

Liu P, Li Y (2011) New species and new records of dictyostelids from Ukraine Mycologia **103**:641–645

Liu P, Li Y (2017) Dictyostelids from Jilin Province, China II. Phytotaxa **323**:077–082

Liu P, Zou Y, Hou J, Stephenson SL, Li Y (2019a) *Dictyostelium purpureum* var. *pseudosessile*, a new variant of dictyostelid from tropical China. BMC Evol Biol **19**:78

Liu P, Zou Y, Li S, Stephenson SL, Wang Q, Li Y (2019b) Two new species of dictyostelid cellular slime molds in high-elevation habitats on the Qinghai Tibet Plateau, China. Sci Rep **9**:5

Liu P, Zou Y, Li W, Li Y, Li X, Che S, Stephenson SL (2019c) Dictyostelid celluar slime molds from Christmas Island, Indian Ocean. mSphere **4**:e00133-19

Medlin L, Elwood HJ, Stickel S, Sogin M (1988) The characterization of enzymatically amplified eukaryotic 16S-like rRNA-coding regions. Gene **71**:491–499

Olive EW (1901) A preliminary enumeration of the sorophoreae. Proc Am Acad Arts Sci **37**:333–344

Paillet Y, Satre M (2010) The biodiversity of dictyostelids in mountain forests: A case study in the French Alps. Pedobiologia **53**:337–341

Perrigo AL, Baldauf SL, Romeralo M (2013) Diversity of dictyostelid social amoebae in high latitude habitats of Northern Sweden. Fungal Divers **58:**185–198

Romeralo M, Baldauf SL, Cavender JC (2009) A new species of cellular slime mold from southern Portugal based on morphology, ITS and SSU sequences. Mycologia **101**:269–274

Romeralo M, Moya-Larano J, Lado C (2011a) Social Amoebae: Environmental Factors influencing their distribution and diversity across South-Western Europe. Microbial Ecol **61**:154–165

Romeralo M, Landolt JC, Cavender JC, Laursen GA, Balduf SL (2010) Two new species of dictyostelid cellular slime molds from Alaska. Mycologia **102**:588–595

Sheikh S, Thulin M, Cavender JC, Hemandez RE, Kawakami SI, Lado C, Landolt JC, Nanjundiah V, Queller D, Shaap P, Strassmann J, Spiegel F, Stephenson SL, Vadell EM, Baldauf SL (2018) A new classification of the dictyostelids. Protist **169**:1–28

Stamatakis A (2006) RAxML-VI-HPC: maximum likelihood-based phylogenetic analyses with thousands of taxa and mixed models. Bioinformatics **22**:2688–2690

Stephenson SL, Landolt JC, Laursen GA (1991) Cellular slime molds in soils of Alaskan Tundra, U.S.A. Arctic Alpine Res **23**:104–107

Stephenson SL, Landolt JC, Laursen GA (1997) Dictyostelid cellular slime molds from Western Alaska, U.S.A., and the Russian Far East. Arctic Alpine Res **29**:222–225

Stephenson SL, Laursen GA, Landolt JC, Seppelt RD (1998) *Dictyostelium mucoroides* from subantarctic Macquarie Island. Mycologia **90**:368–371

Swanson AR, Shadwick JD, Spiegel HFW (2004) Ecological succession of dictyostelid slime molds on the island of Hawaii. Syst Geogr Plants **74**:67-69

Swanson AR, Vadell EM., Cavender JC (1999) Global distribution of forest soil dictyostelids. J Biogeogr **26**:133–148

Traub F, Hohl HR, Cavender JC (1981) Cellular slime molds of Switzerland. I. Description of new species. Am J Bot **68**:162–171

Vadell E, Cavender JC, Landolt JC, Perrigo AL, Liu P, Stephenson SL (2018) Five new species of dictyostelid social amoebae (Amoebozoa) from Thailand. BMC Evol Biol **18**:198

Vadell EM, Cavender JC, Romeralo M, Edwards SM, Baldauf, Stephenson SL (2011) New species of dictyostelids from Patagonia and Tierra del Fuego, Argentina. Mycologia **103**:101–117

Zhao M, Liu P, An Y, Yao Y, Li Y (2017) *Dictyostelium annularibasimum* (Dictyosteliaceae, Dictyostelida), a new purple species from China. Nova Hedwigia **104**:351–358

Figure legends

Figure 1. (**A**) Map showing the collecting localities in the Russian Far East**.** Korsakovsky District, Sakhalin Island (L1), Dolinsky District, Sakhalin Island (L2), Vladivostok (L3) and Ussuriysk (L4). (**B**) Location of the Russian Far East in relation to the rest of Russia. (**C**) Mixed forest habitat (L1). (**D**) Broadleaf forest habitat (L2). (**E**) Coniferous forest habitat (L1).

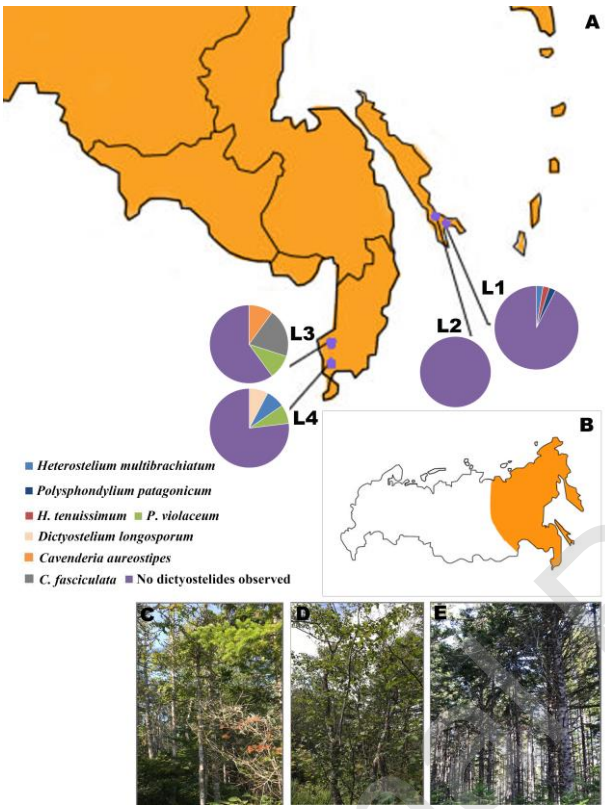

Figure 2. Phylogeny of the seven species obtained in the present study along with other closely related species of dictyostelids, based on SSU rRNA.

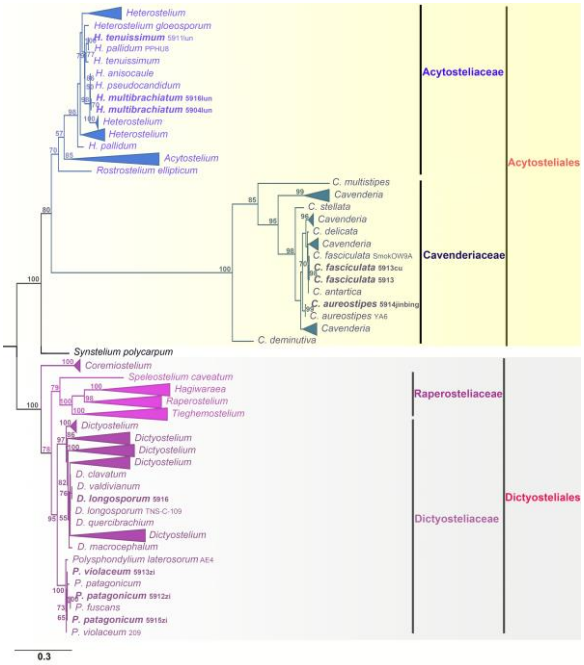

Figure 3. Morphological features of *Heterostelium multibrachiatum*. (**A to C**) Sorocarps. (**D** and **E**) Aggregations. (**F** and **G**) Pseudoplasmodia. (**H**) Sorophore tips. (**I to L**) Sorophore bases. (**M**) Branches. (**N** and **O**) Spores. Bars: A, B, E, F 500 µm; C, G, 200 µm; D, 1 mm; H to O, 20 µm.

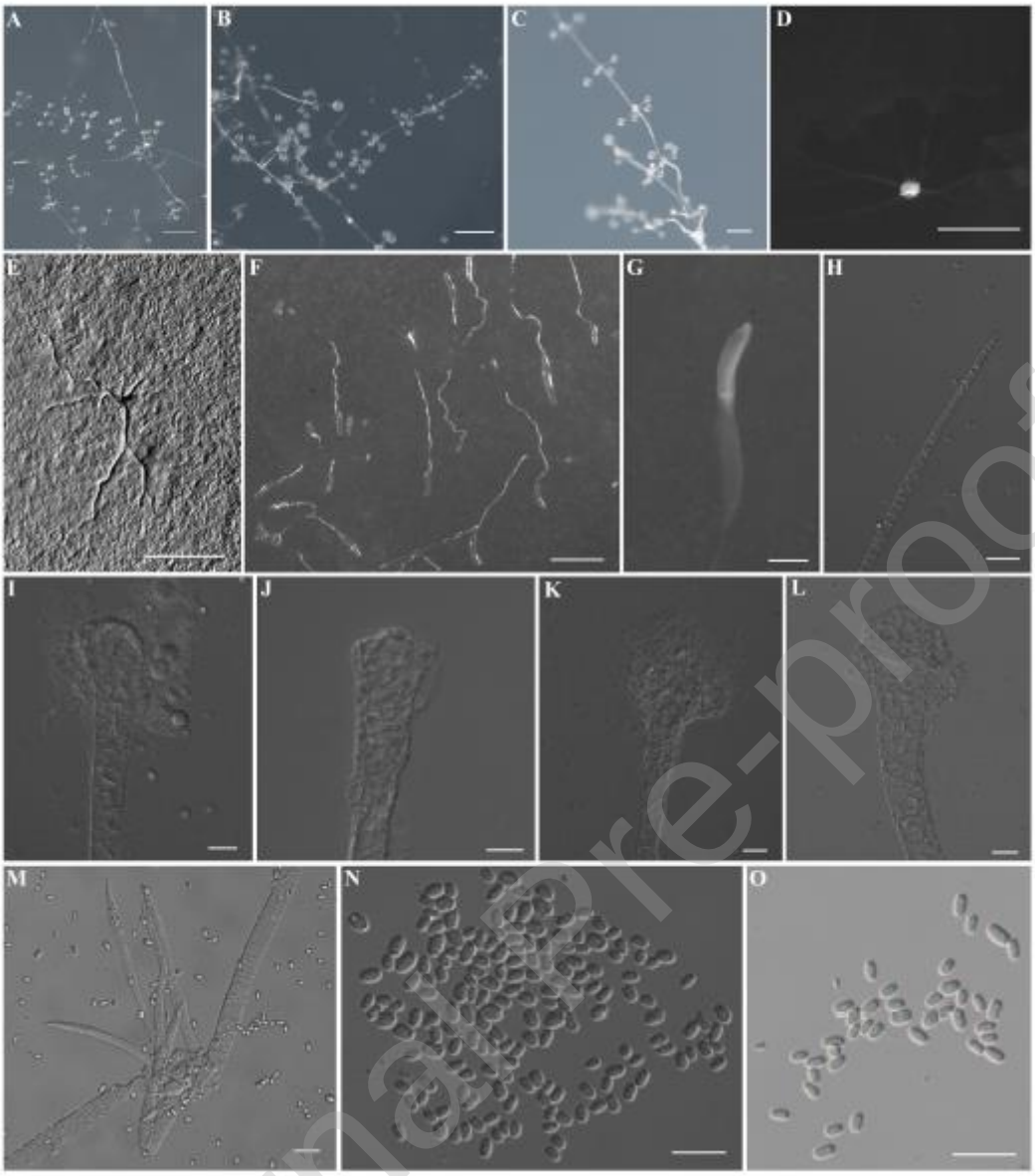

Figure 4. Morphological features of *Polysphondylium patagonicum*. (**A** and **B**) Sorocarps. (**C**) Aggregations. (**D**) Pseudoplasmodia. (**E**) Branches. (**F**) Sorophore tips. (**G**) Sorophore bases. (**H**) Spores. Bars: A, 1 mm; B, 2 mm; C, 200 µm; D, 500 µm; E to H, 20 µm.

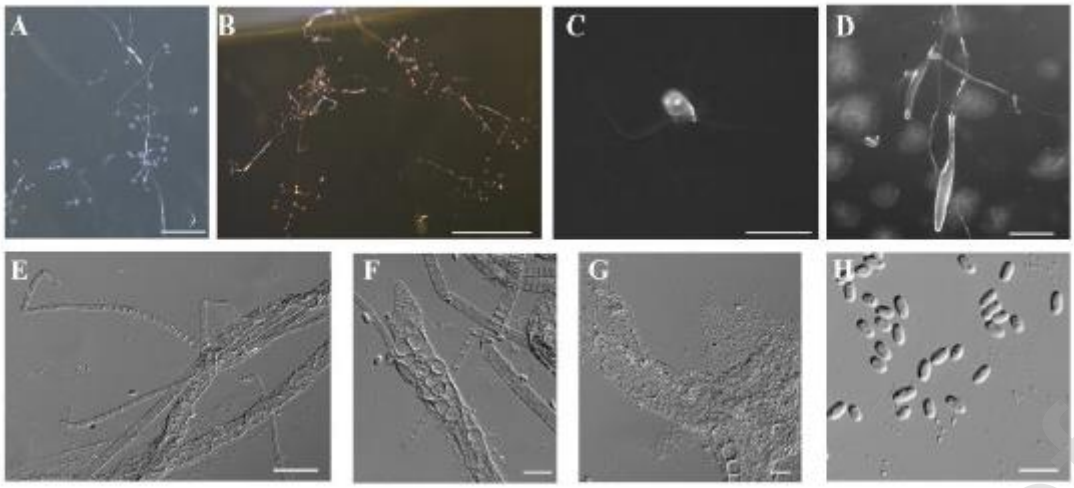

Figure 5. Morphological features of *Cavenderia fasciculata*. (**A** and **B**) Sorocarps. (**C to E**) Aggregations. (**F** and **G**) Pseudoplasmodia and clustered sorogens. (**H**) Sorophore tips. (**I**) Sorophore bases. (**J**) Spores. Bars: A, B, F, G 500 µm; C to E, 1 mm; H to J, 20 µm.

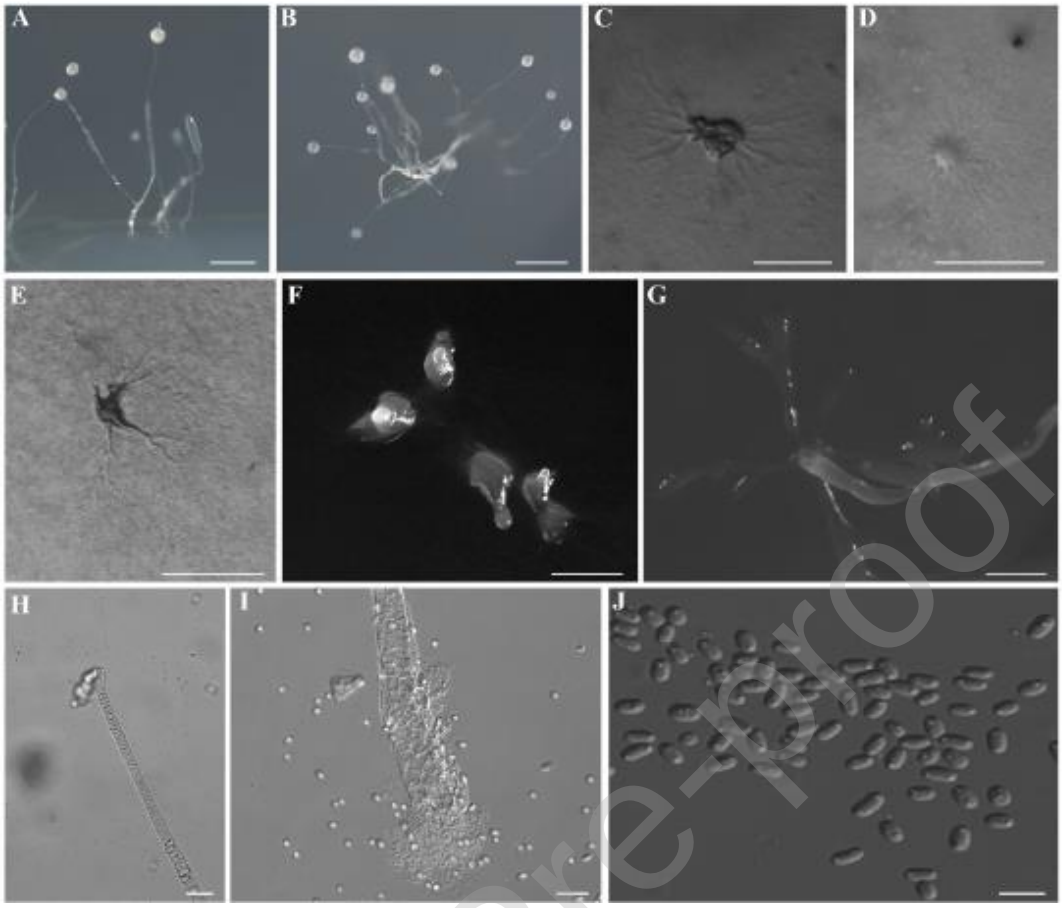

Figure 6. Morphological features of *Heterostelium tenuissimum*. (**A** and **B**) Sorocarps. (**C**) Aggregations. (**D**) Pseudoplasmodia. (**E**) Sorophore tips. (**F** and **G**) Sorophore bases. (**H**) Branches (**I**) Spores. Bars: A, B, D, 1 mm; C, 500 µm; E to I, 20 µm.

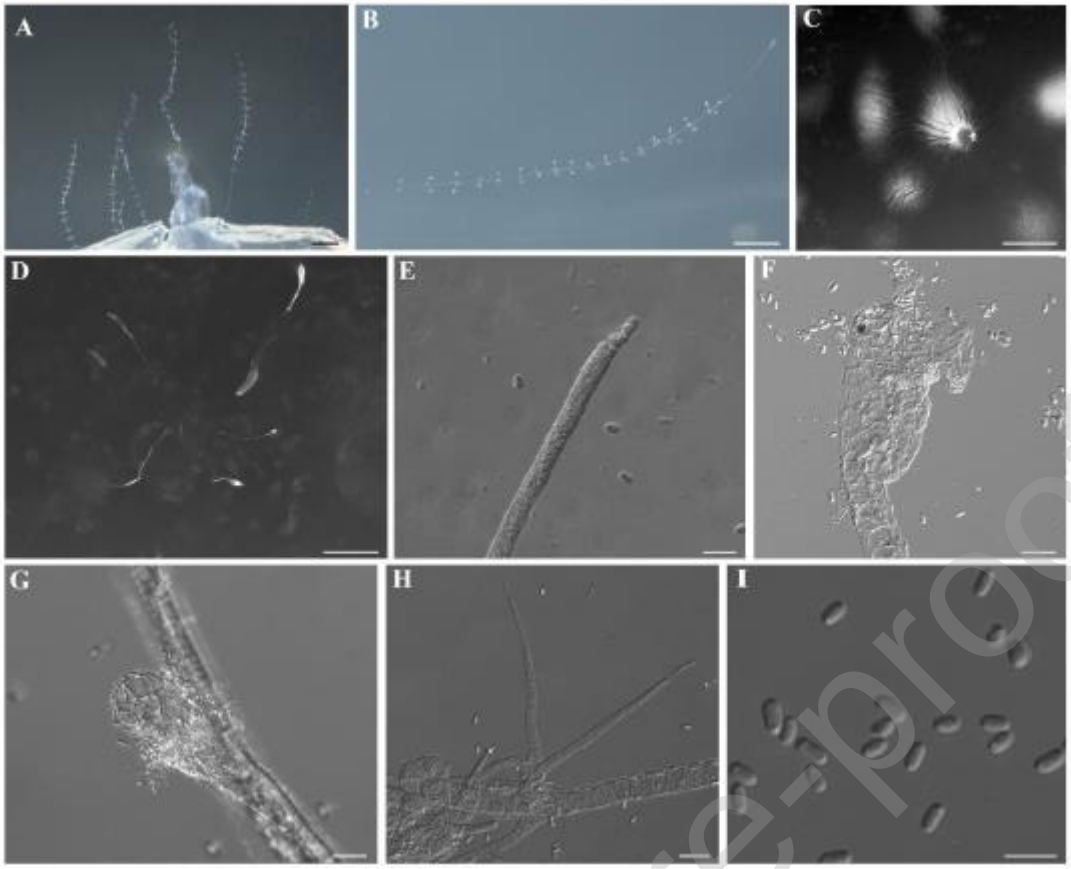

Figure 7. Morphological features of *Dictyostelium longosporum*. (**A** and **B**) Sorocarps. (**C**) Aggregations. (**D**) Pseudoplasmodia. (**E**) Sorophore tips. (**F**) Sorophore bases. (**G**) Spores. Bars: A, D, 1 mm; B, 500 µm C, 5 mm; E to G, 20 µm.

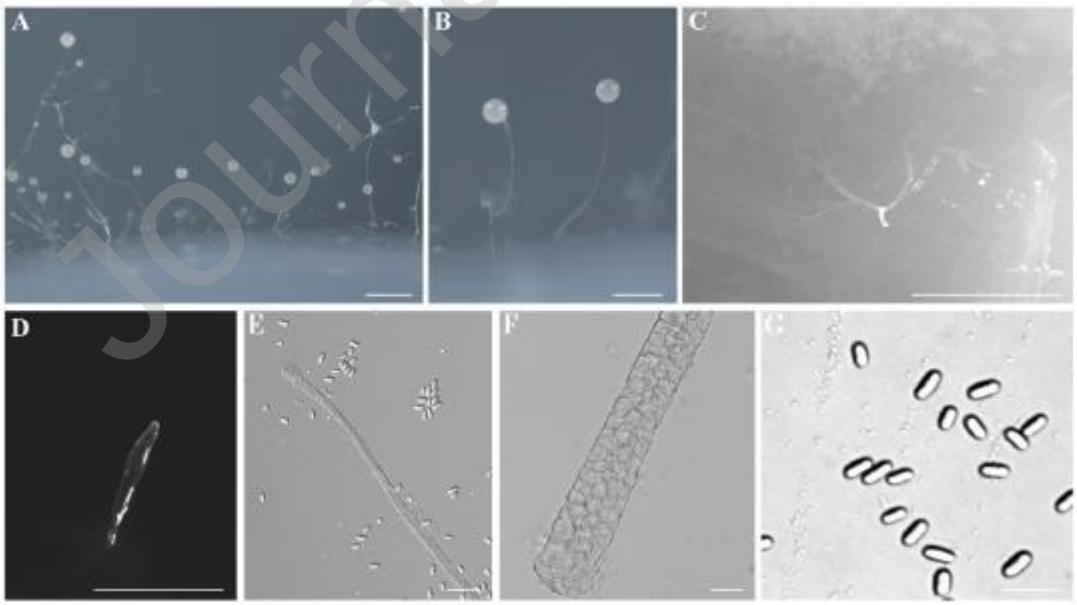

Figure 8. Morphological features of *Polysphondylium violaceum*. (**A to C**) Sorocarps. (**D**) Aggregations. (**E**) Pseudoplasmodia. (**F** and **J**) Sorophore tips. (**G** and **H**) Sorophore bases. (**I**) Branches. (**K**) Spores. Bars: A, C, D, E 1 mm; B, 500 µm; F to K, 20 µm.

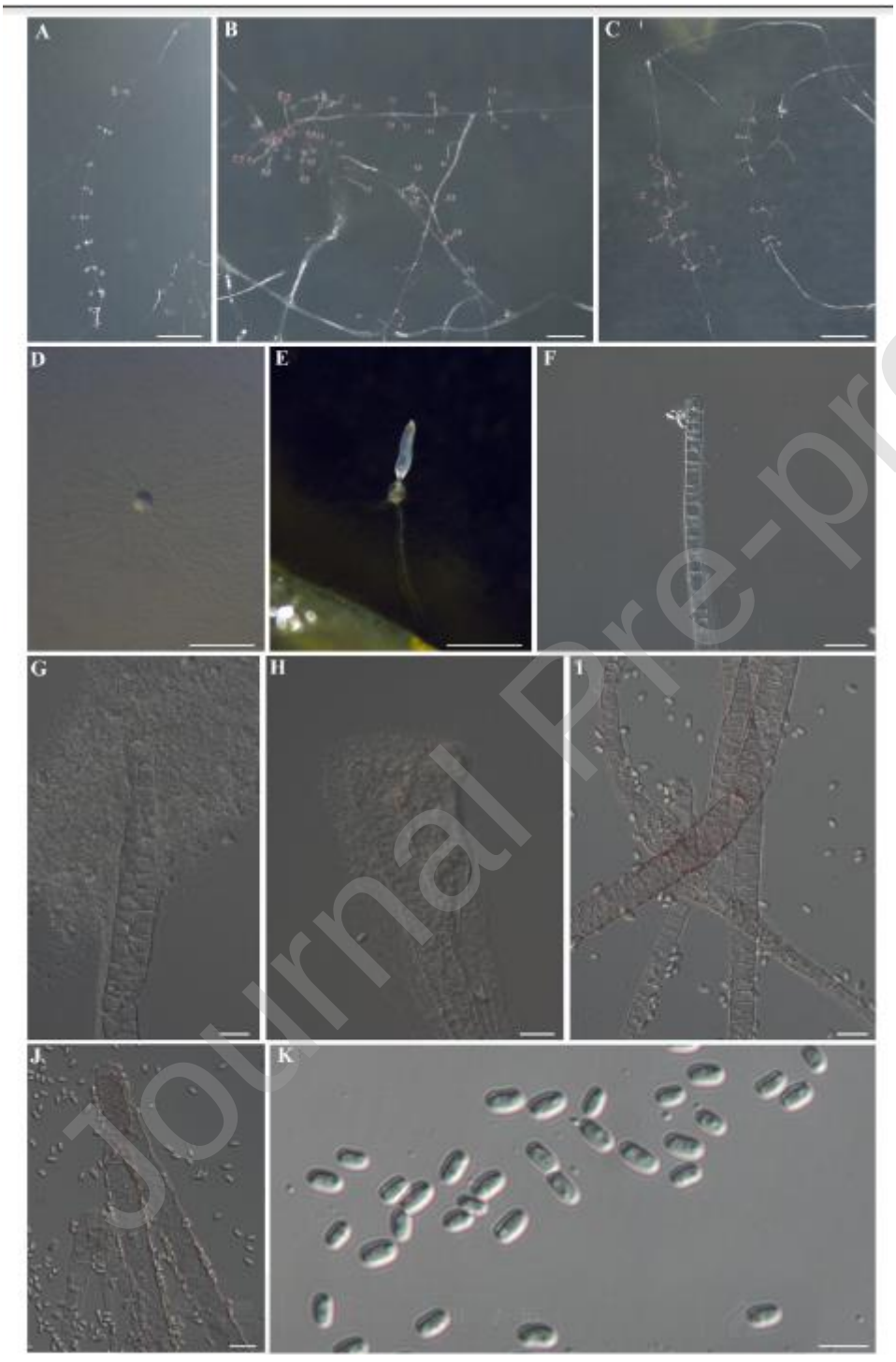

Figure 9. Morphological features of *Cavenderia aureostipes*. (**A**) Sorocarps. (**B**) Aggregations. (**C**) Pseudoplasmodia. (**D** and **E**) Sorophore tips. (**F**) Sorophore bases. (**G**) Spores. Bars: A, 1mm; B, 2 mm ; C, 500 µm; D to G 20 µm.

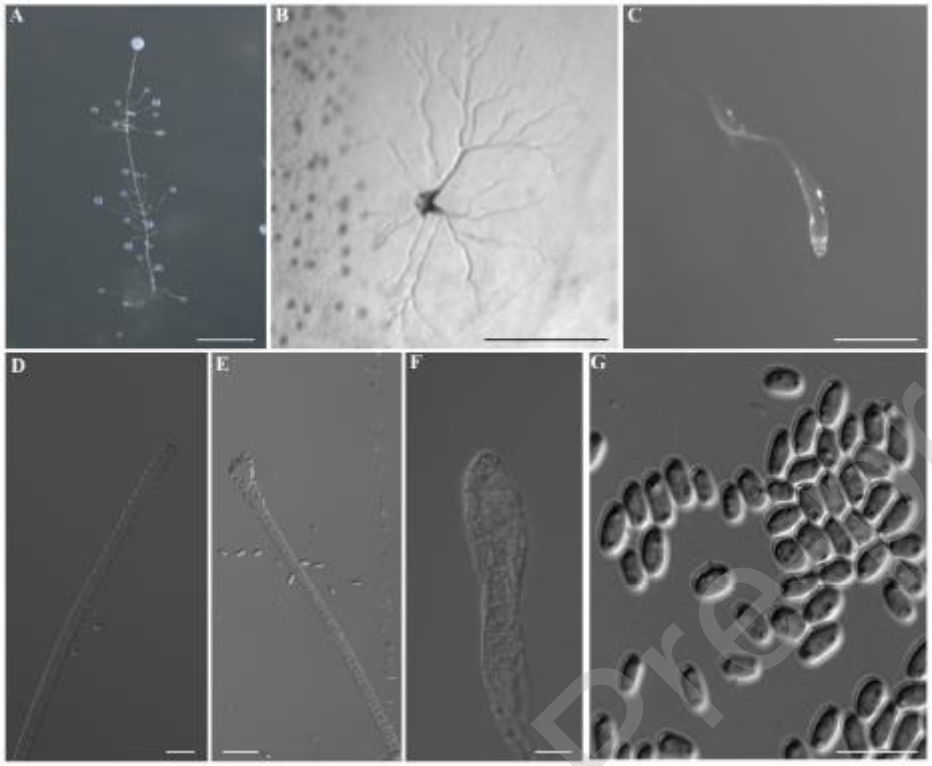

Table legends

Table 1. List of species of dictyostelids isolated from samples collected in the Russian Far East in the present study.

Table 2. NCBI GenBank accession information for SSU sequences of all isolates included in the phylogenetic analysis. New sequences are indicated in bold.

Table 1 List of species of dictyostelids isolated from samples collected in the Russian Far East in the present study.

Soil sample	Locality	Coordinates	Elevation (m)	Habitat	pH	Species of dictyostelid
S5903	Korsakovsky District, Sakhalin Island (L1)	46°63'01''N, 143°20'65''E	-10	mixed forest	5.33	—
S5904	Korsakovsky District, Sakhalin Island (L1)	46°83'07''N, 143°17'05''E	2.5	mixed forest	4.45	***Heterostelium multibrachiatum*
S5905	Korsakovsky District, Sakhalin Island (L1)	46°77'21''N, 143°34'08''E	3.8	mixed forest	6.01	—
S5906	Korsakovsky District, Sakhalin Island (L1)	46°82'03''N, 143°22'01''E	-0.6	mixed forest	5.66	—
S5907	Korsakovsky District, Sakhalin Island (L1)	46°83'08''N, 143°17'04''E	3.2	mixed forest	6.14	—
S5908	Dolinsky District, Sakhalin Island (L2)	47°37'04''N, 142°80'07''E	-0.9	broadleaf forest	6.22	—
S5909	Dolinsky District, Sakhalin Island (L2)	47°27'03''N, 142°75'08''E	16.7	mixed forest	5.78	—

S5910	Korsakovsky District, Sakhalin Island (L1)	46°83'07''N, 143°17'05''E	-3	coniferous forest	6.03	—
S5911	Korsakovsky District, Sakhalin Island (L1)	46°60'05''N, 143°18'09''E	-3	coniferous forest	5.81	**H. tenuissimum*
S5912	Korsakovsky District, Sakhalin Island (L1)	46°59'09''N, 143°18'05''E	17.7	coniferous forest	5.35	**Polysphondylium patagonicum*
S5913	Vladivostok, Primorsky Krai (L3)	43°19'37''N, 131°92'12''E	52	mixed forest	6.12	**Cavenderia fasciculata* (2); *P. violaceum*
S5914	Vladivostok, Primorsky Krai (L3)	43°19'37''N, 131°92'12''E	52	mixed forest	6.85	*C. aureostipes*
S5915	Ussuriysk, Primorsky Krai (L4)	43°69'04''N, 132°15'46''E	184.4	mixed forest	7.08	*P. violaceum*
S5916	Ussuriysk, Primorsky Krai (L4)	43°69'43''N, 132°15'29''E	100.9	mixed forest	7.06	**Dictyostelium longosporum*; ***H. multibrachiatum*

* Refers to a species new to Russia

** Refers to a species new to science

(2) Indicates that two isolates of this species were obtained from this soil sample.

Table 2 NCBI GenBank accession information for SSU sequences of all isolates included in the phylogenetic analysis. New sequences are indicated in bold.

Taxon	Isolate no.	Accession no.	Taxon	Isolate no.	Accession no.
Acytostelium amazonicum	HN1B1	HQ141511.1	*C. aureostipes*	YA6	AM168083.1
A. anastomosans	PP1	AM168115.1	*C. boomerangispora*	K26B	HQ141520.1
A. digitatum	OH517	AM168114.1	*C. delicata*	TNS-C-226	AM168093.1
A. leptosomum	212rjb	HQ141512.1	*C. deminutiva*	MexM19A	AM168092.1
A. longisorophorum	DB10A	AM168109.1	*C. exigua*	TNS-C-199	AM168085.1
A.magnisorum	08A	HQ141513.1	*C. fasciculata*	SmokOW9A	AM168086.1
A. serpentarium	SAB3A	AM168113.1	***C. fasciculata***	**5913**	**MN752220**
A. singulare	FDIB	HQ141514.1	***C. fasciculata***	**5913cu**	**MN752221**
A. subglobosum	LB1	AM168110.1	*C. granulophora*	CHII-4	AM168072.1
Cavenderia antarctica	NZ43B	AM168080.1	*C. macrocarpa*	MGE2	HQ141519.1
C. amphispora	BM9A	HQ141521.1	*C. medusoides*	OH592	AM168088.1
C. aureostipes	**5914jinbing**	**MN752226**	*C. mexicana*	MexTF4B1	AM168089.1
C. microspora	TNS-C-38	AM168090.1	*D. clavatum*	TNS-C-220	AM168035.1

C. multistipes	UK26b	AM168070.1	*D. crassicaule*	93HO-33	AM168037.1
C. myxobasis	NT2A	HQ141522.1	*D. dimigraformum*	AR5b	AM168038.1
C. parvispora	OS126	AM168091.1	*D. discoideum*	NC4	AM168071.1
C. stellata	SAB7B	AM168081.1	*D. firmibasis*	TNS-C-14	AM168041.1
Coremiostelium polycephalum	MY1-1	AM168056.1	*D. giganteum*	WS589	AM168042.1
C. polycephalum	Landolt #1130 SS3B	HQ141488.1	*D. intermedium*	PJ11	AM168044.1
C. polycephalum	MY1-1	AM168056.1	*D. implicatum*	93HO-1	AM168043.1
Dictyostelium ammophilum	MR-2009b KBK4A	HQ141478.1	*D. longosporum*	TNS-C-109	AM168048.1
D. aureum	SL1	AM168028.1	***D. longosporum***	**5916**	**MN752223**
D. aureocephalum	TNS-C-180	AM167876.1	*D. leptosomum*	NZN49A	HQ141480.1
D. barbibulus	Sweden-4R	JX173878.1	*D. macrocephalum*	B33	AM168049.1
D. brefeldianum	TNS-C-115	AM168030.1	*D. medium*	TNS-C-205	AM168050.1
D. brunneum	WS700	AM168031.1	*D. mucoroides*	TNS-C-114	AM168053.1
D. capitatum	91HO-50	AM168032.1	*D. purpureum*	C143	AM168060.1
D. citrinum	OH494	AM168033.1	*D. pseudobrefeldianum*	91HO8	AM168059.1
D. quercibrachium	NZ201B	HQ141479.1	*H. candidum*		AY040337.1
D. robustum	TNS-C-219	AM168064.1	*H. candidum*	bsb6b	HQ141498.1

D. rosarium	M45	AM168065.1	*H. colligatum*	HN13C1	HQ141505.1
D. septentrionale	AK2	AM168067.1	*H. equisetoides*	B7JB	AM168099.1
D. sphaerocephalum	GR11	AM168068.1	*H. filamentosum*	SU-1	AM168100.1
D. valdivianum		GQ496155.1	*H. flexuosum*	AU4B	HQ141500.1
Hagiwaraea coeruleostipes	CRLC53B	AM168036.1	*H. gloeosporum*	TCK52	AM168074.1
H. lavandula	B15	AM168047.1	*H. granulosum*	MF5A	HQ141502.1
H. radiculata	ML5A	HQ141494.1	*H. lapidosum*	ALP-2015c	KP167477.1
H. rhizopodium	AusKY-4	AM168063.1	*H. luridum*	LR-2	AM168101.1
H. vinaceofusca	CC4	AM168062.1	*H. migratissimum*	ALP-2015d	KP167481.1
Heterostelium ampliverticillatum	ALP-2015a	KP167480.1	***H. multibrachiatum***	**5916lun**	**MN752217**
H. anisocaule	NZ47B	AM168096.1	***H. multibrachiatum***	**5904lun**	**MN752217**
H. arachnoideum	YA1	AM168102.1	*H. multicystogenum*	AS2	HQ141506.1
H. asymetricum	HN20C	HQ141503.1	*Heterostelium oculare*		HQ141497.1
H. australicum	NB1AP	HQ141508.1	*H. pallidum*	PPHU8	EU004605.1
H. boreale	MR-2009a	HQ141499.1	*H. pallidum*	TNS-C-98	AM168103.1
H. parvimigratum	ALP-2015e	KP167483.1	***P. violaceum***	**5915zi**	**MN752225**
H. pseudocandidum	TNS-C-91	AM168107.1	*Raperostelium australe*	NZ80B	AM168029.1
H. pseudocolligatum	ALP-2015g	KP167474.1	*R. capillare*	MR-2011c	JF892721.1

H. pseudoplasmodiofascium	ALP-2015h	KP167482.1	*R ellipticum*	AM168112.1	AE2
H. pseudoplasmodiomagnum	ALP-2015i	KP167472.1	*R. filiforme*	MR-2011e	JF892724.1
H. racemiferum	ALP-2015j	KP167476.1	*R. gracile*	TNS-C-183	AM168078.1
H. rotatum	QC2C	HQ141501.1	*R. ibericum*	214rjb	HQ141495.1
H. tenuissimum		AY040339.1	*R. maeandriforme*	MR-2011f	JF892719.1
H. tenuissimum	**5911lun**	**MN752222**	*R. minutum*	71-2	AM168051.1
H. tikalense	OH595	AM168106.1	*R. monochasioides*	HAG653	AM168052.1
H. unguliferum	ALP-2015k	KP167473.1	*R. ohioense*	Okla4C	HQ141493.1
H. violaceotypum	ALP-2015l	KP167478.1	*R. potamoides*	FP1A	AM168069.1
Polysphondylium fuscans	Sweden-11D	JX173877.1	*R. reciprocatum*	MR-2011i	JF892718.1
P. laterosorum	AE4	AM168046.1	*R. tenue*	Pan52	AM168076.1
P. patagonicum		GQ496156.1	*Synstelium polycarpum*	VE1b	AM168057.1
P. patagonicum	**5912zi**	**MN752219**	*Tieghemostelium angelicum*	MR-2011a	JF892716.1
P. violaceum	209	HQ141486.1	*T. dumosum*	MR-2011d	JF892722.1
P. violaceum	**5913zi**	**MN752224**	*T. lacteum*		AM168045.1
T. menorah	M1	AM168073.1	*T. unicornutum*	MR-2011l	JF892725.1
T. montium	MR-2011h	JF892717.1	*Speleostelium caveatum*	WS695	AM168077.1
T. simplex	MR-2011j	JF892720.1			